Cavitation-Erosion-Induced Phase Transformations in Alloys

D. A. WOODFORD

Previously reported surface phase transformations occurring during cavitation erosion in cobalt- and iron-base alloys have been confirmed. However, an examination of the effect of aging treatments on Stellite 6B failed to demonstrate any simple relationship between transformation characteristics and erosion resistance. For several iron-base transformable alloys, the erosion resistance was shown to be related to strength and again no direct correlation could be established between transformation and erosion. It is concluded that the phase transformation is incidental to the erosion process. However, since many erosion resistant alloys do undergo a deformation-induced phase transformation, a more general explanation for the erosion resistance of alloys with close-packed structures is offered in terms of stacking fault energy.

EROSION by liquid impingement or cavitation is an extremely important technological problem which so far has received little attention from metallurgists. Whenever a component is subjected to impingement by liquid drops at high relative velocities, or cavitation in a liquid at the solid interface resulting from rapid changes in pressure, a progressive loss of material from the surface will occur. The most commonly cited examples of the two types of erosion in practice are the impingement attack of condensed water droplets on last stage steam turbine buckets and cavitation erosion of ship propellers. In the former case it is common practice to shield the leading edges of the buckets with a strip of an erosion resistant cobalt-base alloy.

There is considerable evidence that the progress of material loss is similar in both cases.[1] For example, an incubation period during which deformation of the surface occurs accompanied by little or no material loss is commonly observed in all erosion situations. Consequently, a study of cavitation erosion which is more convenient to perform, is believed to be relevant to an understanding of impingement attack.

Many attempts have been made to correlate erosion resistance with mechanical properties such as hardness, fatigue resistance or strain energy (some measure of the area under a stress-strain curve). However, none of these has been very satisfactory. The slopes and position of hardness vs erosion resistance curves differ appreciably for different materials or alloy types.[2] Cobalt-base alloys, in particular, frequently show exceptional erosion resistance at moderate hardness levels. Similarly, correlations with strain energy are poor when applied to a wide range of materials.[2,3] For specific materials there appears to be some connection between erosion resistance and fatigue properties.[4] Fatigue-like striations have been observed on eroded surfaces,[4,5] but no general correlations have been made.

It is clear, therefore, that attempts to relate erosion resistance to some readily measurable mechanical property have so far failed to provide any real insight into the erosion problem. What is needed is a comprehensive description of the microstructural changes resulting from erosion to account for the fundamentally different response among different materials. For example, the cobalt alloy Stellite 6B has a steady-state rate of volume loss an order of magnitude less than many titanium- and iron-base alloys of comparable hardness.[5]

It has been reported recently[6] that Stellite 6B and other cobalt alloys undergo a stress-induced phase transformation during cavitation erosion. Although it is well known that the fcc phase may transform to hcp during deformation of many cobalt alloys,[7,8] the work of Gould[6] demonstrated a close association between the progress of cavitation erosion and the surface transformation. This phase transformation has been confirmed in dilute Co-Fe alloys[9] and, in addition, a new hexagonal phase with a four-layer stacking sequence, designated η was discovered. Phase transformations have also been observed by several Russian authors[10,11] during erosion testing of metastable austenitic alloys. Since these alloys also have a relatively high erosion resistance, it has been speculated that the phase transformation in cobalt alloys[6] and in austenitic alloys[10,11] is continuously absorbing a portion of the cavitation energy.

The present work was designed to examine the role of the phase transformation in detail using surface X-ray analysis and metallography. Although the previously reported experimental observations are confirmed and extended, the present observations now cast considerable doubt on the idea that the phase transformation is directly responsible for a high resistance to erosion.

MATERIAL AND PROCEDURE

Haynes Stellite alloy 6B was received in the form of mill-annealed sheet (2250°F, rapid air cool). The chemical composition in weight percent was: 27.6Cr, 5.08W, 1.05C, 2.51Ni, 1.40Fe, 1.05Mn, 0.33Mo, 0.15Si. In addition to testing in the as-received condition, the effect of various aging treatments was studied.

To examine the phase transformation in iron-base alloys, several high strength TRIP[12] steels were

tested. These steels were processed by rolling up to 90 pct at temperatures between 480° and 840°F. All the steels are fully austenitic at room temperature but transform partly to martensite during deformation. In these alloys a reasonable estimate of austenite stability during tensile testing is given by the transformation coefficient, m, as defined by

$$V\alpha = m\epsilon^{1/2}$$

where $V\alpha$ is the volume fraction of bcc martensite and ϵ is the engineering strain. Thus the value of m provides a measure of the extent of transformation for a given amount of strain. The composition, tensile properties, values of m and the approximate M_D temperatures (the temperature above which no transformation occurs during deformation) as given by Gerberich[13] are listed in Tables I and II. Steel 5 was obtained from a separate source and values of m and M_D were not available. Several 300 series metastable steels were additionally tested for comparison.

The ultrasonic cavitation apparatus used in this work and the specimen details have been described extensively elsewhere.[5] A Branson ultrasonic signal generator provides a constant frequency 20,000 Hz signal to an air-cooled piezoelectric crystal. The strain amplitude output of the crystal is then amplified by an exponential horn which carries a threaded specimen with a circular $\frac{1}{2}$ in. diam head fitting flush with the horn tip. For the present work, since the alloys were received in sheet form, $\frac{1}{2}$ in. diam by $\frac{1}{16}$ in. thick disks were brazed (Stellite) or soldered (iron-base alloys) onto specimen dummies made from an austenitic iron-base alloy (A-286). The maximum brazing temperature was about 1200°F.

The amplitude of vibration at the specimen tip was measured with an optical microscope focussed on a transverse scratch at the tip. For the particular horn geometry used, a range of amplitudes between 9×10^{-4} and 2.1×10^{-3} in. was obtained with a measurement precision of about $\pm 3 \times 10^{-4}$ in. Nominal amplitudes between 10^{-3} and 2×10^{-3} in. were used in the present study.

Table I. Chemical Composition of TRIP Steels, Wt Pct

Steel No.	Cr	Ni	Mn	Mo	Si	C	N
1	8	--	13	--	--	--	0.21
2	8	--	13.5	--	--	0.26	--
3	11.2	8	0.4	1.9	0.1	0.27	--
4	9	7.4	2.9	4.0	2.8	0.24	--
5	9.47	8.41	2.08	3.56	2.16	0.29	--

Table II. Tensile and Transformation Characteristics of TRIP Steels

Steel No.	Y.S., psi	UTS, psi	Elong, Pct	m	M_D, °F
1	172000 (2)	187000	42	~0.95	~185
2	216000 (1)	245000	7.6	<0.5	~122
3	210000 (2)	235000	47	~1.8	~338
4	231000 (2)	243000	32	~1.3	~230
5	215000 (1)	268000	31	–	–

(1) 0.2 pct offset.
(2) yield point.

The specimen surface was initially prepared by standard metallographic procedures followed by a light electrolytic etch. Testing was performed by immersing the horn tip with the specimen attached in a water-cooled bath of deionized water maintained at a temperature of $52° \pm 2°F$. The test is started by setting the power supply to give the required amplitude of vibration at the specimen surface. Rapid pressure changes at the specimen surface lead to the generation and subsequent violent collapse of bubbles resulting in cavitation attack which is monitored throughout the test by periodic weight loss measurements. Optical microscopy was used to record the surface changes in the initial stages and X-ray diffractometer patterns were obtained periodically to measure the percentage phase transformation using CoKα radiation and an iron filter. For the cobalt alloy the phase percentages were calculated on the basis of the diffracted intensities for $\{10\bar{1}1\}_{hcp}$ and $\{200\}_{fcc}$ according to the equation derived by Sage and Guillaud:[14]

$$\text{wt pct hcp} = \frac{I\{10\bar{1}1\}_{hcp} \times 100}{I\{10\bar{1}1\}_{hcp} + 1.5\ I\{200\}_{fcc}}$$

This equation takes into consideration both structural and multiplicity factors but does not adequately correct for the size effect of the very thin hcp platelets or for the effects of lattice strains caused by cold work.[8]

In the iron-base alloys, both ϵ and α martensite were detected after erosion. A rough measure of the amounts of each phase present was obtained by comparing peak intensities. The absolute accuracy of these values is not known but is likely to be poor, particularly when three phases are present, because these heavily worked alloys have a strong preferred orientation. Nevertheless, there were pronounced differences in the transformation characteristics of the alloys so that the procedure could be justified for qualitative comparison.

RESULTS AND DISCUSSION

A) Cobalt Alloy – Stellite 6B

The initial objective was to confirm the previous observations on the progress of transformation in this alloy.[6] Fig. 1 shows the weight loss vs time and the corresponding transformation behavior during erosion at a nominal vibration amplitude of 0.001 in. An initial incubation period during which the weight loss is small corresponds to a rapid increase in the pct hcp phase present. After about 15 hr the weight loss rate becomes constant and the transformation maintains a reasonably constant level of about 65 pct. A probable explanation for this behavior is that during the incubation period the surface is deforming with an associated deformation-induced transformation up to a critical amount at which point local fracture and particle separation occurs. This exposes softer untransformed material which is then capable of deformation up to the critical amount. Thus, a steady-state rate of weight loss corresponds with the establishment of a constant level of transformation. A similar pattern is observed at a higher amplitude of 0.0017 in., Fig. 2, with a considerably less pronounced incubation period and a more extensive transformation approaching 80 pct. Of interest here is the periodic variation in the

Fig. 1—Weight loss and phase transformation characteristics for Stellite 6B as functions of test time at an amplitude of 0.001 in.
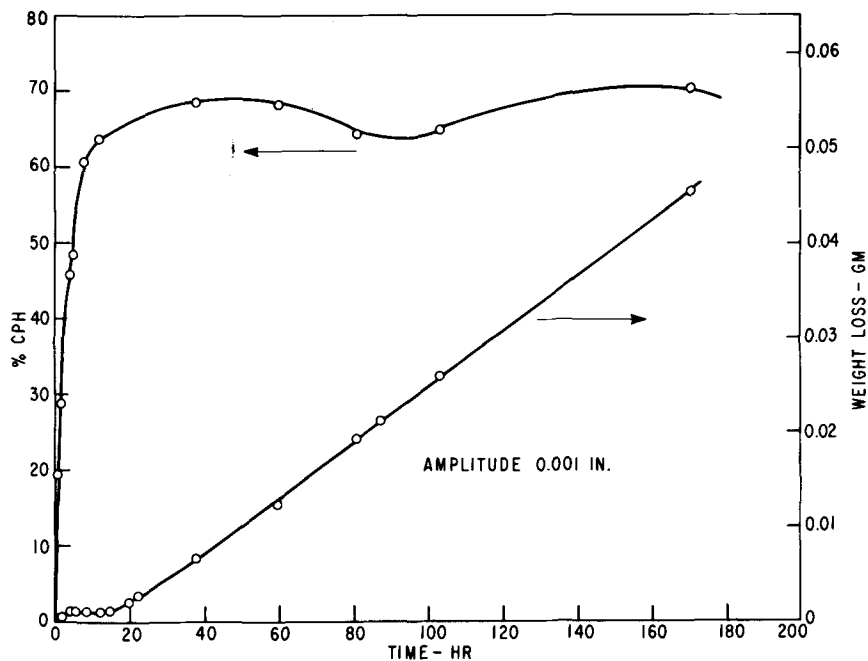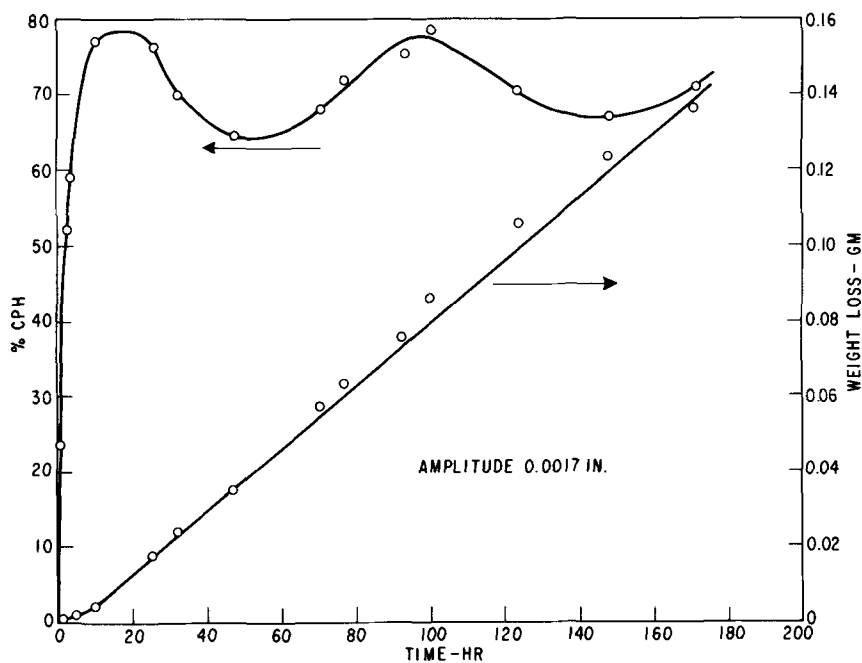

Fig. 2—Weight loss and phase transformation characteristics for Stellite 6B as functions of test time at an amplitude of 0.0017 in.

amount of transformation with time. This variation is also apparent in Fig. 1 at a reduced frequency and amplitude of cycle. The mechanism responsible for this behavior has not been determined. However, it is probably related to the morphology of erosion attack in the specimens used. Initial material loss occurs in a narrow rim about $\frac{1}{16}$ in. inside the specimen periphery and then advances towards the center. Whereas the weight loss curve relates to the total erosion attack, the X-ray beam was focussed on the center portion of the specimen. If, in fact, the attack progresses in periodic waves moving from the outside to the specimen center, the X-ray measurements would be expected to reflect this behavior.

By successive grinding and polishing of the eroded surface, the transformed layer was found to extend to a depth between 1 and 2×10^{-3} in. Fig. 3 is a cross-

section of the eroded specimen used to construct Fig. 2. The transformation markings may be seen in both bright field and plane polarized light confirming the measured depth of transformation. Since the X-ray beam penetrates about 5×10^{-4} in., it is possible that the measured amount of transformation is to some extent a reflection of the depth of transformation in addition to the total amount transformed at the eroding surface.

Having confirmed that the phase transformation occurs, it became necessary to determine whether the erosion resistance could be directly related to either the rate or amount of transformation. Clearly, the amount of transformation (or depth as discussed above) increases at the higher vibration amplitude but this is to be expected as a result of the more severe surface deformation. To establish a possible direct relation-

ship between erosion resistance and transformation, the Stellite 6B was given various heat treatments to change the erosion resistance.

Fig. 4 compares the weight loss curve for the as-received condition with those obtained for specimens given additional aging treatments for 24 hr at 1400°, 1700°, and 2000°F. Aging at 2000°F has no significant effect on erosion whereas aging at lower temperatures results in considerable loss in erosion resistance. It is of interest to note that the hardest condition (R_C-46 after aging at 1400°F compared with R_C-39 in the mill-annealed condition) had the worst response. This is contrary to normal behavior for a given class of alloys although other exceptions have been reported.[2] The corresponding transformation characteristics are shown in Fig. 5. Differences in the rate and amount of transformation for the mill-annealed specimen and that given an age at 2000°F are not reflected in the weight loss curves. Moreover, the transformation characteristics of the three aged specimens are almost identical suggesting that the differences in Fig. 4 cannot be attributed to any gross measure of the tendency to transform.

Figs. 6 and 7 compare the surface changes up to the approximate end of the incubation period for the two extremes in aging temperature and erosion resistance. In Fig. 6, the transformation markings of the hcp phase are apparent after 2 hr. Material loss from the matrix occurs initially at the ϵ platelet interfaces and develops by further loss in the matrix and at the M_7C_3 carbides. Although X-ray diffraction indicated 100 pct fcc after aging at 2000°F, Fig. 7 suggests some transformation in the original condition. This develops progressively with increasing test time. One important difference in this specimen is that erosion of the carbide appears to be more rapid than erosion of the
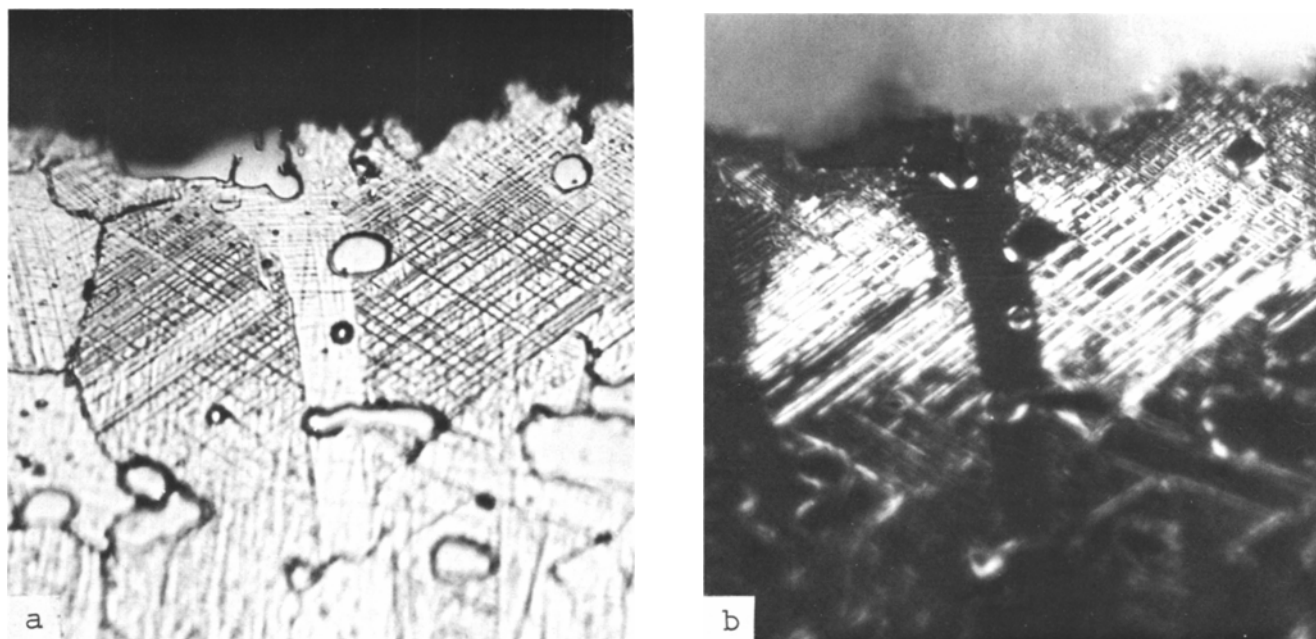

Fig. 3—Transverse section showing depth of transformation after 170 hr at 0.0017 in. amplitude. (a) Bright field. (b) Polarized light. Etched 5HCl − 4 CrO₃ (10 pct), magnification 1000 times.
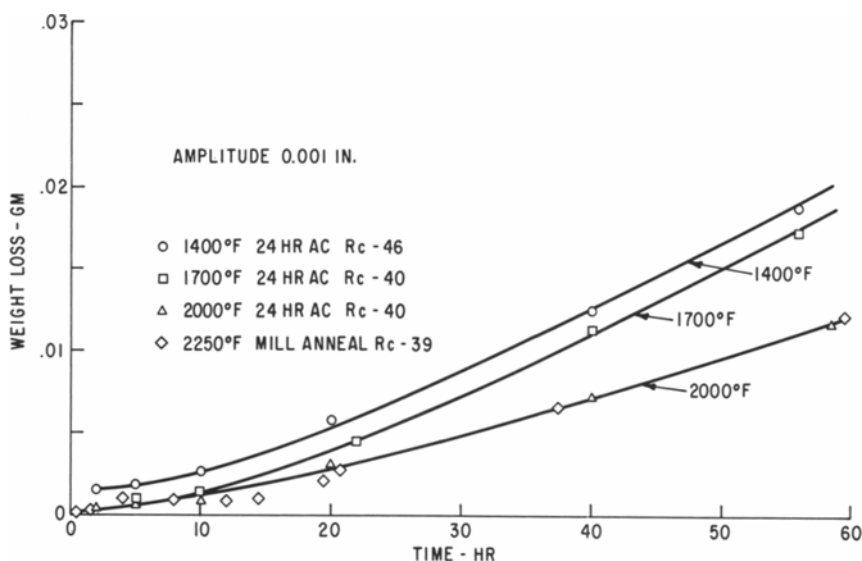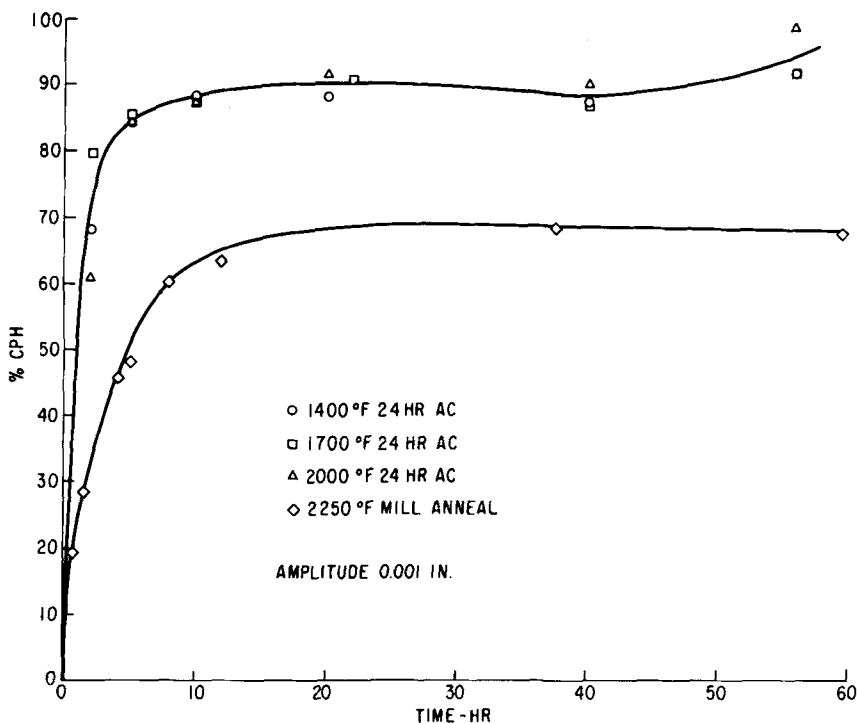

AMPLITUDE 0.001 IN.

o 1400°F 24 HR AC Rc - 46
□ 1700°F 24 HR AC Rc - 40
△ 2000°F 24 HR AC Rc - 40
◇ 2250°F MILL ANNEAL Rc - 39

Fig. 4—Effect of aging on erosion of Stellite 6B.

Fig. 5—Effect of aging on transformation characteristics in Stellite 6B.

o 1400 °F 24 HR AC
□ 1700 °F 24 HR AC
△ 2000 °F 24 HR AC
◇ 2250 °F MILL ANNEAL

AMPLITUDE 0.001 IN.

matrix. The two large carbide particles on the left and right of the field have been extensively eroded after 10 hr whereas the matrix is far less damaged than that in the harder specimen aged at 1400°F and subjected to the same exposure.

Stellite 6B is more likely to transform to hcp phase than most cobalt-base alloys since the fcc stabilizing elements iron and manganese are present in small amounts. Although carbon has a strong stabilizing effect in solution,[15] most of it may be tied up as a carbide. In fact, by suitable heat treatment, partial transformation may be achieved by thermal exposure alone.[16] This discovery presented the possibility of measuring the erosion resistance of the alloy as a function of the initial amount of hcp phase. Fig. 8 shows the weight loss curves after three different heat treatments.* The standard mill-annealed condition is

*These data were taken from a different machine at a nominal amplitude of 0.002 in. Although reproducibility on any one machine is excellent, considerable variability between machines has been observed. Thus the weight loss rate for the mill-annealed condition is slightly less than that in Fig. 2 at a nominal amplitude of 0.0017 in. This can be accounted for by a variation between machines equivalent to the estimated precision of calibration of ±3 × 10⁻⁴ in.

additionally annealed at 2250°F for 2 hr and water quenched producing a measured 3.5 pct hcp, believed to result from the deformation associated with quenching stresses. The third treatment is similar to that used by Derow and Bleil[16] and involves a conditioning treatment at 1650°F to precipitate most of the carbon and a subsequent isothermal exposure at 1250°F for 200 hr. This treatment resulted in 28 pct hcp. Further details are given in Fig. 8. It is clear that the erosion resistance is not significantly affected by the amount of hcp present initially. A possible marginal increase in weight loss for the third treatment may be attributed to the slight increase in hardness. Aging at 1400°F does increase the hardness and reduce the erosion resistance, Fig. 4. These data suggest, as in the aging experiments, that the phase transformation is not directly

responsible for the erosion resistance. They imply that the hcp phase has a similar erosion resistance to that of the fcc phase.

B) Iron-Base Alloys

The weight loss curves for the five TRIP steels are shown in Fig. 9. Also included is the curve for Stellite 6B* and type 301 stainless steel in the annealed con-

*Comparison on the basis of volume loss would lower this curve slightly because of the greater density of Stellite 6B.

dition with a tensile strength of about 90,000 psi. Even the highest strength TRIP steel is inferior to Stellite 6B. Fig. 10 is a plot of weight loss after 50 hr as a function of tensile strength and a rather good correlation is obtained for the TRIP steels. This curve extrapolates to the range for Stellite 6B at a strength level of 300,000 psi. However, the cobalt alloy has an actual strength of about 150,000 psi demonstrating its inherent superiority in terms of erosion resistance to strength ratio. Type 301 stainless steel (and also types 303 and 304 which have similar erosion resistances but are omitted from Fig. 9 for clarity) has excellent erosion resistance for its strength level.

The transformation characteristics for all the steels tested are summarized in Table III. With the reservation already discussed regarding the absolute accuracy of these data, clear differences are indicated. The steels stabilized with manganese (1 and 2) transform partly to nonmagnetic, hcp, ε martensite. The other three TRIP steels stabilized with nickel transform various amounts to α martensite. The stainless steels show different amounts of ε and α martensites.
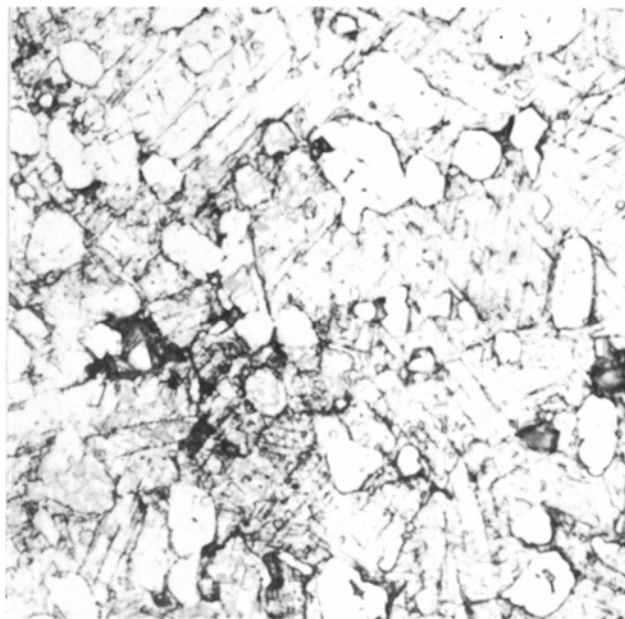
The progress of transformation in TRIP 5 is compared with the weight loss measurements in Fig. 11. Although the incubation stage is less clearly defined, the pattern of behavior is similar to that of Stellite 6B, Figs. 1 and 2. However, the data in Table III do not
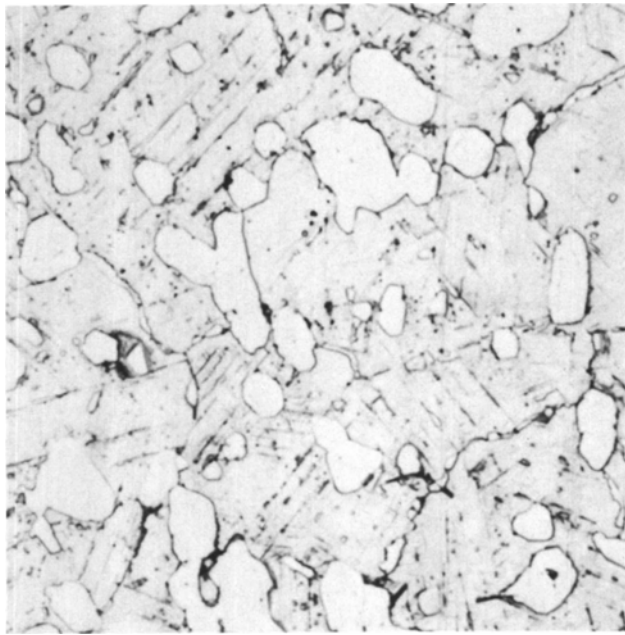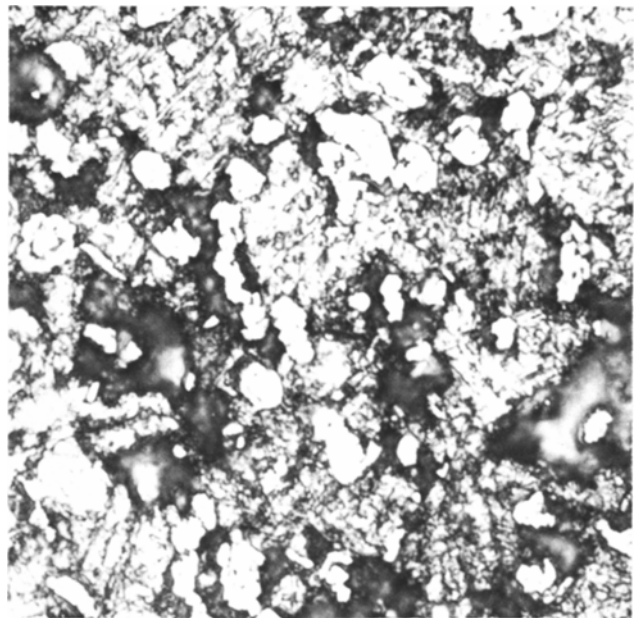
(a)
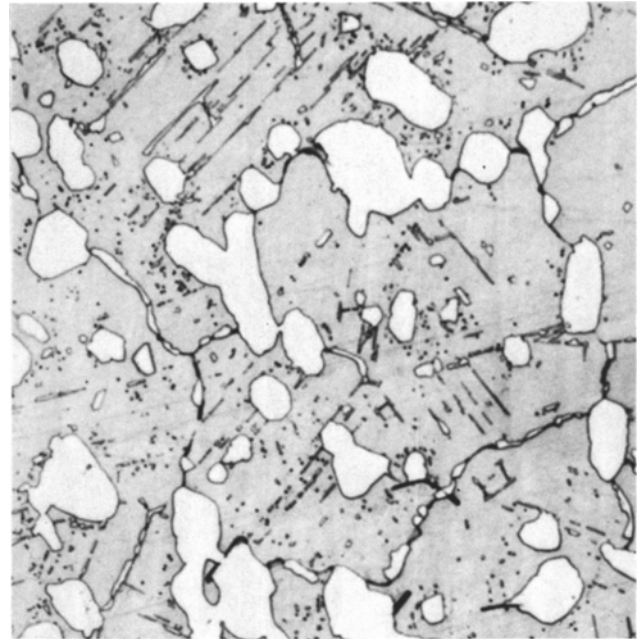
(b)

(c)

(d)

Fig. 6—Initial erosion characteristics in Stellite 6B at 0.001 in. amplitude. Aged 1400°F, 24 hr, magnification 1000 times. (a) Original; (b) 2 hr; (c) 5 hr; (d) 10 hr.

suggest any simple relationship between erosion resistance and transformation. The erosion resistance seems to be determined mainly by the tensile strength for each class of steel. Comparison between the TRIP steels and the stainless steels indicates that the latter are inherently superior (i.e. they give comparable erosion resistance at much lower strength levels).

There is no apparent relationship between the measured transformation, Table III, or the m value or M_D temperature, Table II, and the erosion resistance of the TRIP steels. Alloy 2 with the lowest values of m, M_D, and elongation had relatively good erosion resistance comparable with alloy 3 with the highest value of m, M_D, and elongation. This substantiates the lack of correlation between transformation and erosion resistance observed for Stellite 6B. The reason for inherent

Table III. Summary of Erosion Resistance and Transformation Characteristics for Iron-Base Alloys

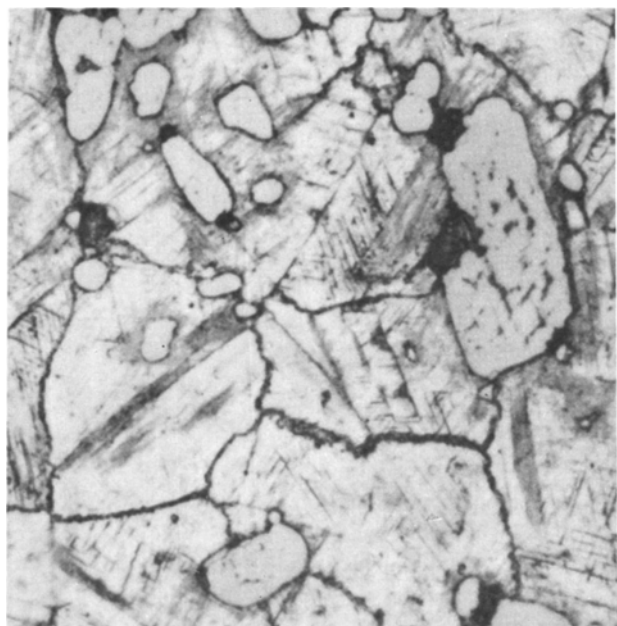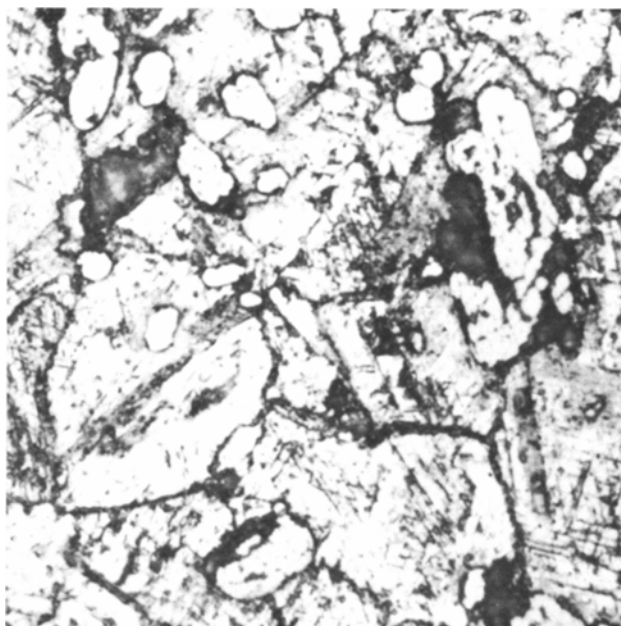| Steel	Tensile Strength, ksi	Weight Loss After 50 Hr, gm	Percentage Transformation After 10 hr	
			α-Martensite	ε-Martensite
TRIP 1	187	0.124	30	30
2	245	0.031	–	6
3	235	0.034	65	–
4	243	0.046	Trace	–
5	268	0.022	30	–
Type 301	90*	0.063	91	2
303	65*	0.099	53	13
304	70*	0.070	83	–

*Estimated from hardness measurements.

(a)
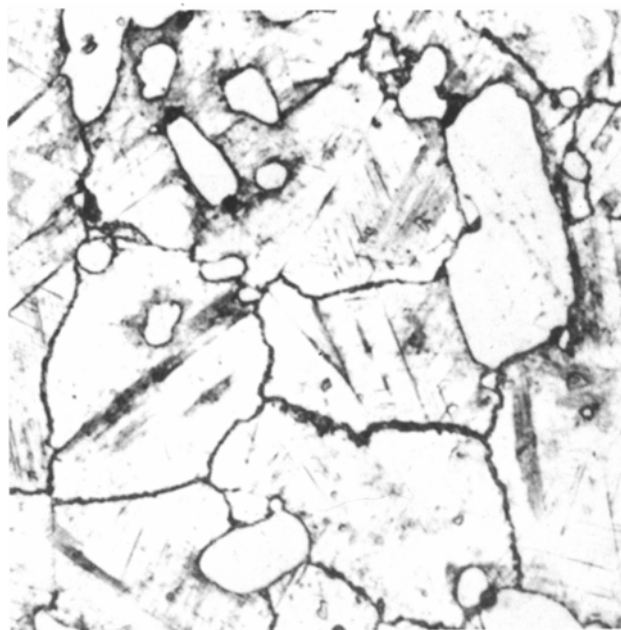
(b)

(c)

(d)

Fig. 7—Initial erosion characteristics in Stellite 6B at 0.001 in. amplitude. Aged 2000°F, 24 hr, magnification 1000 times. (a) Original; (b) 2 hr; (c) 5 hr; (d) 10 hr.

Table IV. Transformation Data for Co-Fe Alloys

	Pct FCC	
Wt Pct Fe	Initial	After 10 hr
2	1	0
5	98.5	14
15	100	100

differences between alloy types at comparable strength levels remains to be determined.

DISCUSSION

It now seems clear that, although many erosion-resistant materials do undergo a surface phase trans-formation during cavitation erosion, no direct corre-lation can be established. A recent study[9] of Co-Fe alloys containing 2, 5, and 15 wt pct Fe gives further support to this conclusion. The erosion resistance de-creased progressively with increasing iron. Measured phase percentages before starting the test and after 10 hr erosion are reproduced in Table IV. This shows that the alloy which was initially almost entirely hcp had the highest erosion resistance.

The lack of correlation between erosion resistance and any simple measure of transformation suggests that any contribution from the transformation in ab-sorbing some of the energy associated with the cavita-tion process is likely to be minor. Nevertheless, the fact remains that these transformable alloys do have high erosion resistance relative to non-transformable

fcc alloys. An alternative interpretation of their erosion resistance is therefore proposed in terms of stacking fault energy. It is believed that a reduced S.F.E. leading to planar slip increases the number of cycles to nucleate a crack in high-cycle fatigue compared with a higher S.F.E. material deforming by wavy slip.[17] This could account for reported correlations between high-cycle fatigue strength and erosion resistance.[4] It also enables a rationalization to be made of the observation that the hcp phase in cobalt alloys appears to be as erosion resistance as the fcc phase. This follows from the observation that the two forms

have about the same S.F.E. at the allotropic temperature in pure cobalt.[18] It is also possible to account for the increasing erosion resistance at comparable strength levels for fcc alloys in the order of aluminum-base, copper-base, iron-base.[2] This would be the order expected for decreasing S.F.E.[19]

Although many factors are likely to determine the erosion resistance of a particular alloy so that no detailed interpretation of the present results in terms of variations in S.F.E. can be made, the suggestion that a low S.F.E. favors high erosion resistance seems reasonable. It has one outstanding advantage over the transformation hypothesis, viz. it appears to rank non-transformable alloys in the correct order of erosion resistance. This therefore provides a more general qualitative interpretation and may reflect both crack initiation and work hardening characteristics.

Since, as S.F.E. decreases, the possibility of transformation is likely to increase, the phase transformation may be considered as incidental rather than instrumental in controlling erosion resistance.
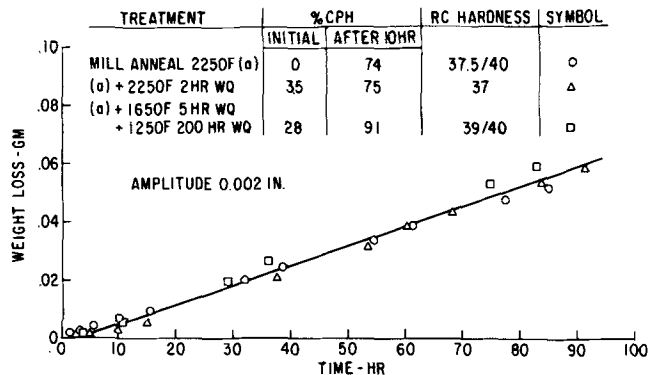
ACKNOWLEDGMENTS

Fig. 8—Erosion resistance of Stellite 6B after heat treatment to give different starting percentages of hcp phase.
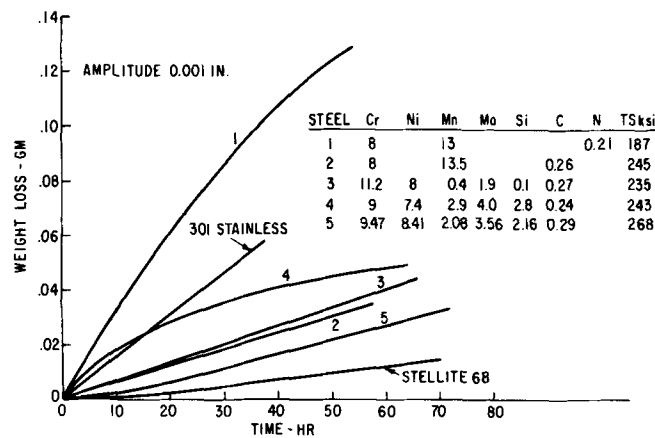

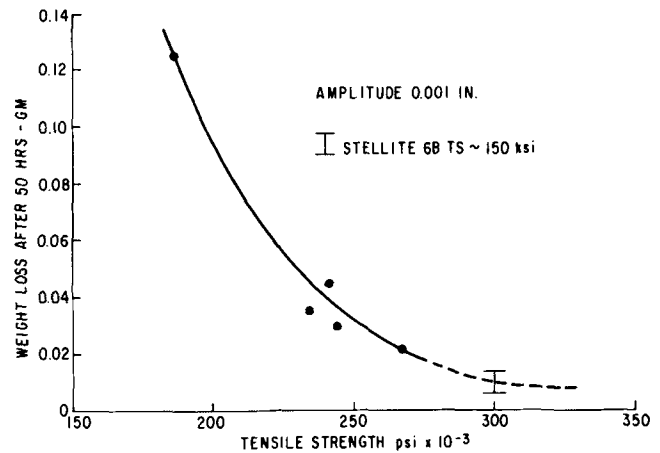Fig. 9—Erosion resistance of transformable steels compared with that of Stellite 6B.
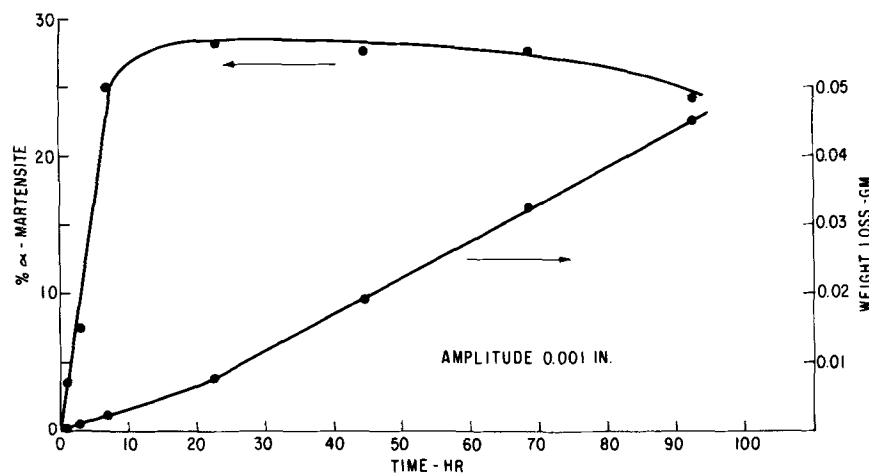

Fig. 10—Weight loss vs tensile strength for TRIP steels.

Fig. 11—Transformation to α − Martensite in TRIP 5.

REFERENCES

1. F. J. Heymann: *Machine Design,* 1970, Dec. 10, p. 118.
2. F. J. Heymann: *Amer. Soc. Test. Mater., Spec. Tech. Publ.* 474, 1970, p. 212.
3. F. G. Hammitt, *et al.: Amer. Soc. Test. Mater., Spec. Tech. Publ.* 474, 1970, p. 288.
4. G. P. Thomas and J. H. Brunton: *Proc. Roy. Soc.,* 1970, vol. A314, p. 549.
5. G. C. Gould: *Amer. Soc. Test. Mater., Spec. Tech. Publ.* 474, 1970, p. 182.
6. G. C. Gould: Presented at *Third Int. Conf. on Rain Erosion and Associated Phenomena,* England, to be published.
7. A. H. Graham: *Trans. ASM,* 1969, vol. 62, p. 930.
8. A. H. Graham and J. L. Youngblood: *Met. Trans.,* 1970, vol. 1, p. 423.
9. D. A. Woodford and H. J. Beattie: *Met. Trans.,* 1971, vol. 2, p. 3223.
10. V. M. Zamoruyev, Y. Y. Zobachev, and A. V. Kartyshov: *Mashinostroenie,* 1965, vol. 12, p. 112.
11. V. V. Fomin and I. Kazarnovskaya: *Stahl,* 1967, no. 4, p. 337.
12. V. F. Zackay, E. R. Parker, D. Fahr, and R. Busch: *Trans. ASM,* 1967, vol. 60, p. 252.
13. W. Gerberich: Dept. of Metallurgy, University of Minnesota, 1970.
14. M. Sage and Ch. Guillaud: *Rev. Met.,* 1950, vol. 47, p. 139.
15. W. Köster: *Z. Metallk.,* 1952, vol. 43, p. 297.
16. H. Derow and H. E. Bleil: NASA Rep. No. Cr-1590, 1970.
17. C. Laird and C. E. Feltner: *Trans. TMS-AIME,* 1967, vol. 239, p. 1074.
18. T. Ericsson: *Acta Met.,* 1966, vol. 14, p. 853.
19. P. C. J. Gallagher: *Met. Trans.,* 1970, vol. 1, p. 2429.